Astron. Astrophys. 360, L17–L20 (2000)

ASTRONOMY
AND
ASTROPHYSICS

LETTER

Letter to the Editor

Multi-layer accretion disks around black holes and formation of a hot ion–torus

A. Hujeirat and M. Camenzind

Landessternwarte-Königstuhl, Königsstuhl 12, 69117 Heidelberg, Germany

Received 17 May 2000 / Accepted 15 July 2000

Abstract. We present the first 2D steady-state numerical radiative hydrodynamical calculations showing the formation of a low-density hot torus in the very inner region of accretion disks around a black hole. The inner part of the disk is found to be thermally unstable when Bremsstrahlung is the dominant cooling mechanism. Within the parameter regime used and in the absence of magnetic fields, the torus-plasma is highly time-dependent with supersonic oscillating motion with respect to the electron temperature.

When the soft photons from the disk comptonize the electrons efficiently, the ion-pressure supported torus shrinks in volume, but decelerates further the inward motion into the hole. We speculate that magnetic fields would stabilize the tori by lowering its energy package through initiating jets and/or outflows.

In the outer region, we find that the scale height of the angular velocity H_Ω largely exceeds the scale height of the density H_ρ. This yields a multi-layer flow-structure in the vertical direction which slows the inwards motion into the BH significantly, enhancing further the formation of the hot torus.

Key words: Black holes - Accretion disks – Boundary layers – relativistic hydrodynamics – Radiation

1. Introduction

Recent theoretical studies of disk accretion under low accretion rates onto compact objects have been modeled in one–dimensional vertically integrated hydrodynamical approaches by Narayan & Yi (1994), known as advection–dominated accretion flows (ADAF), or more recently as advection–dominated accretion flows including outflows (ADIOS, Blandford & Begelman 1999, see also Abramowicz et al. 2000). The 1+1D vertical structure of the disk using the two-temperature description has also been recently studied by $Różańska$&Czerny (2000). Time–dependent hydrodynamical simulations of accretion flows onto compact objects in higher dimensions are now accessible using high performance supercomputers (Hawley 2000, Igumenshchev&Abramowicz 2000, Igumenshchev et al. 2000). 2D time–dependent simulations performed to model the very inner region of the disk are usually hampered by short integration times, which only can cover a few inner rotational periods of the order of a fraction of a millisecond for stellar mass objects. This is by far too short to test the behaviour of disks on time–scales of the order of at least a few seconds (i.e. thousands of dynamical time–scales), as shown in the temporal structure of the X–ray emission.

Such long time–scales are only accessible by means of time–implicit algorithms. The simulations presented here are based on the time–implicit Newtonian radiative MHD solver IRMHD (Hujeirat 1998). In order to mimic the relativistic nature of the central object, gravity is included in terms of the quasi–Newtonian potential of Paczynski & Wiita (1980).

In this letter, we report on the first results from such simulations which completely resolve the vertical structure. As a first result we find a new branch of solutions with a topology not confirming one–dimensional calculations.

2. Time–implicit axisymmetric accretion flows

Under axi-symmetry, the hydrodynamical equations consist of the continuity equation for the density, Euler's equations for three momenta, two equations for the internal energies of the ions and electrons, and one equation for the energy density of the radiation field. The equation of the radiative density is solved using the flux–limited diffusion (FLD) (Pomraning & Levermore 1981). The opacity is modified so that the radiation-matter collisional term $\Lambda_{\rm B} \doteq \kappa\rho(T^4 - E)$ reduces to pure Bremsstrahlung $\rho^2 T^{1/2}$ in optically thin regions and to the radiative diffusion operator for higher optical depths.

Gravity of the central object is described in terms of the quasi–Newtonian potential of Paczynski & Wiita (1980). In all models, we assume a 3 $M_\odot$ central black hole, and an accretion rate of $-\dot{\mathcal{M}} = 10^{16}{\rm g\,s}^{-1}$ is set to enter the domain $D = [0 \leq \theta \leq \pi/2] \times [1 \leq r \leq 10]$ via a thin disk across the outer boundary. The accretion flow will be followed down to some radius within the marginal stable orbit, where GR–effects become important. We have set this inner radius as $R_{\rm in} = 2.8\,R_{\rm S}$, where $R_{\rm S}$ denotes the Schwarzschild radius

Send offprint requests to: A. Hujeirat

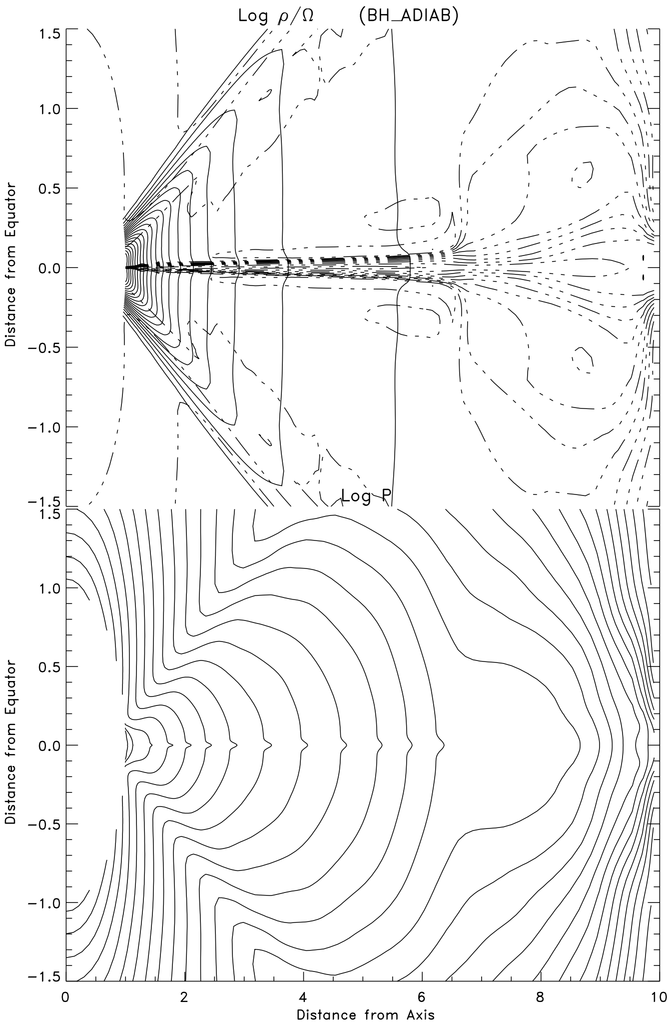

Fig. 1. Equi–distant contour–lines of density ρ and angular velocity Ω (dashed and solid lines, top), and of the pressure P (bottom) in accretion onto a black hole of $3\ M_{\odot}$ after 2000 orbital periods (in units of the orbital period of the marginal stable orbit). A material flux $-\dot{\mathcal{M}} = 10^{16}\,\mathrm{g\,s^{-1}}$ is set to enter the domain of integration through the outer boundary. The distances from the axis and the equator are in units of $2.8\,R_{\mathrm{S}}$. This model is adiabatic in the sense that the dissipated energy is assumed to be radiated away instantaneously.

$R_{\mathrm{S}} = 2GM/c^2$. All radii are given in the following in units of R_{in}.

Although the solutions sought are initial-conditions-independent, we mention them here for completeness. We split D into the disk region $D_{\mathrm{disk}} = [0 \le \theta \le \theta_{\mathrm{d}}] \times [1 \le r \le 10]$ and a corona region $D_{\mathrm{C}} = D - D_{\mathrm{disk}}$, where $\theta_{\mathrm{d}} = H/r$ and H denotes the classical thickness of the disk.

In D_{disk} the matter is set to rotate keplerian with $\Omega_{\mathrm{K}}(r,\theta) = GM/r(r - R_S)$, and we set the density $\rho(r,\theta) = \rho(10,\theta) = \rho_0 \times \max(\mathrm{e}^{-(\mathrm{z/H})^2}, 10^{-4})$ and $T(r,\theta) = T(10,\theta) = T_0$, where $dz = r\,d\theta$ and the sub-script '0' denotes the corresponding equatorial value at the outer boundary. In D_{C} we set $\Omega = 0$, $\rho(r,\theta) = 10^{-4}\,\rho_0$, $T(r,\theta) = T_{\mathrm{Virial}}$. The poloidal component of the velocity field in D is set to vanish.

Since we are interested in steady configurations and since the flow is viscous and ρ in D_{C} is not sufficiently small, we have found that an unreasonably large shear $(\partial V/\partial\theta)$ along the inner boundary shows up whenever a non-rotating cold corona is considered. Therefore, the actual advantageous of incorporating a corona is to reduce the shear and to keep the Mach numbers along R_{in} comparable.

Across the inner boundary, free-fall for the radial velocity and stress–free conditions for the angular velocity are imposed. Normal symmetry and anti–symmetry conditions are assumed along the equator and along the polar axis. The domain of integration is divided into 200×70 strongly stretched finite volume cells in the radial and vertical directions, respectively. Following Shapiro et al. (1975, SLE), the ions are heated via turbulent dissipation and the electrons cool via Bremsstrahlung and comptonization, where the disk is the only source of soft photons. For dynamical viscosity we use $\eta_{\mathrm{t}} = \rho\nu_{\mathrm{t}} = \rho\alpha\, V_{\mathrm{S}}^{\mathrm{Eq}} H$ as the turbulent diffusion coefficient. $V_{\mathrm{S}}^{\mathrm{Eq}} = V_{\mathrm{S}}(r, \theta = 0)$ is the equatorial–plane value of the sound speed and $H = \epsilon r$, where $\epsilon = 0.0083$ and $\alpha = 0.1$.

The calculations proceed as follows. Using the above-mentioned initial conditions and assuming a local balance between turbulent heating $\Gamma = \eta_{\mathrm{t}} D^2$ and cooling Λ, we have carried the calculations till the maximum time-independent residual Res_2 has dropped below a certain small value ϵ_c. In this model, 1200 orbital periods (OPs) have elapsed when Res_2 has dropped below ϵ_{c} for the first time. Since only quasi-stationary solutions have been detected, we carried out the calculations further for additional 800 OPs for sure.

The solutions obtained are then used as initial conditions for the next model. Here we switch on turbulent heating and Bremsstrahlung cooling, and run the calculations for additional 2000 orbital periods within which Res_2 has been verified to drop below ϵ_{c}.

Similarly, the solutions obtained in the later model are used as ICs for the next model, in which Compton cooling is switched on. We stress here that what characterizes the steadiness of our solutions is $Res_2 \le \epsilon_{\mathrm{c}}$ and not the number of orbital periods.

3. Multi–layer structure of hot accretion disks

In standard accretion disks, the thickness is characterized through the pressure scale–height H_{P}. For temperature increasing in the vertical direction, H_{P} largely exceeds the density scale–height H_{ρ}. As in the case of stratified rotating fluids, there will always be mechanisms (magnetic fields, convection, radiation and turbulence) available that guarantee a rotational–coupling of the corona to the disk, resulting in an angular velocity scale–height H_{Ω} that largely exceeds H_{P} (see Fig. 1 and Fig. 3). Consequently, a low–density, hot and rapidly rotating layer between H_{Ω} and H_{P} will show up (see Fig. 1 and Fig. 3). As the viscosity ν_{t} in this layer is smaller than in the disk, the flow is likely to be oppositely oriented to that in the disk (Fig. 5). While using lower viscosity pronounces the multi-layer structure of the disk and subsonically slows the inflow of disk-matter into the hole (see Fig. 2), higher viscosity diminishes the vertical variations and accelerates the inflow across the inner boundary up to the supersonic regime (Hujeirat & Camenzind 2000).

In the two-temperature description, the ion-pressure $P_{\rm i}$ highly exceeds the electron-pressure $P_{\rm e}$ and therefore has a stronger impact on the global flow-behaviour. $P_{\rm e}$, on the other hand, can be viewed as a perturbative source and likely to be comparable to the turbulent pressure $P_{\rm tur}$. Note that this is equivalent to the case when the main source of dissipation is due to magnetic reconnection that primarily heats up the electrons, and subsequently a fraction only goes into heating the ions via modified Coulomb interaction. Therefore, in our present models, we use $T_{\rm e}$ to determine the sound speed in evaluating $\eta_{\rm t}$. This allows supersonic motion to evolve with respect to electron–temperature and still being subsonic with respect to ion–temperature.

Our calculations show that the very inner portion of a thin disk is thermally unstable when Bremsstrahlung is the dominant cooling mechanism. The density in the disk increases inwards down to some critical radius $R_{\rm C}(\geq R_{\rm S})$, below which the gas loses centrifugal support and starts to fall freely inwards, yielding a strong inwards decrease of the density attaining a minimum value right at the inner boundary. In this region

$$\frac{\Lambda_{\rm B}}{\Gamma} \propto \frac{\rho}{T_{\rm e}^{1/2}} \frac{1}{D^2}. \quad (1)$$

Note that while D^2 and $T_{\rm e}$ increase inwards, ρ decreases. Consequently, the disk starts to expand from inside-to-outside forming thereby a hot torus. When switching on Compton cooling and using the two-temperature description, the torus-volume shrinks with the ion-pressure being the main stabilizing force against gravity, similarly to what was proposed by Rees et al. in 1982 (see Fig. 4). Within the torus, a quasi-equilibrium state between the inflow of matter from the disk and outflow from beneath into the BH is established. The dynamics in the torus is highly dominated by supersonic oscillating motions (supersonic with respect to $T_{\rm e}$).

Our calculations with $H = 0.1R$ or with $\eta_{\rm t} = \alpha P_{\rm ions}/\Omega_{\rm K}$ do not hinder the formation of the hot torus, but rather compress its volume further (Hujeirat&Camenzind 2000). Equivalently, increasing the accretion rate will have a similar effect. The torus however disappears if the accretion rate or the turbulent viscosity are sufficiently large and the flow becomes ADAF.

By performing long–term axisymmetric hydrodynamical simulations for accretion flows around a stellar black hole of $3\,M_{\odot}$ at a sub–Eddington accretion rate we found the formation of an inner hot ion–torus extending between the horizon and $\simeq 6\,R_{\rm S}$. Due to the low–density, cooling via Bremsstrahlung and Coulomb interaction between ions and electrons (both $\propto \rho^2$) are no longer effective, so that electrons can cool down by comptonization, explaining in this way the cutoff–energies of $\simeq$ 100 keV for BHLMXBs.

We note that the transition from a cold disk to a hot torus is likely to be sharp (see SLE). We think that including ion- and electron-conduction is likely to smooth this transition, but unlikely to change the above flow topology obtained.

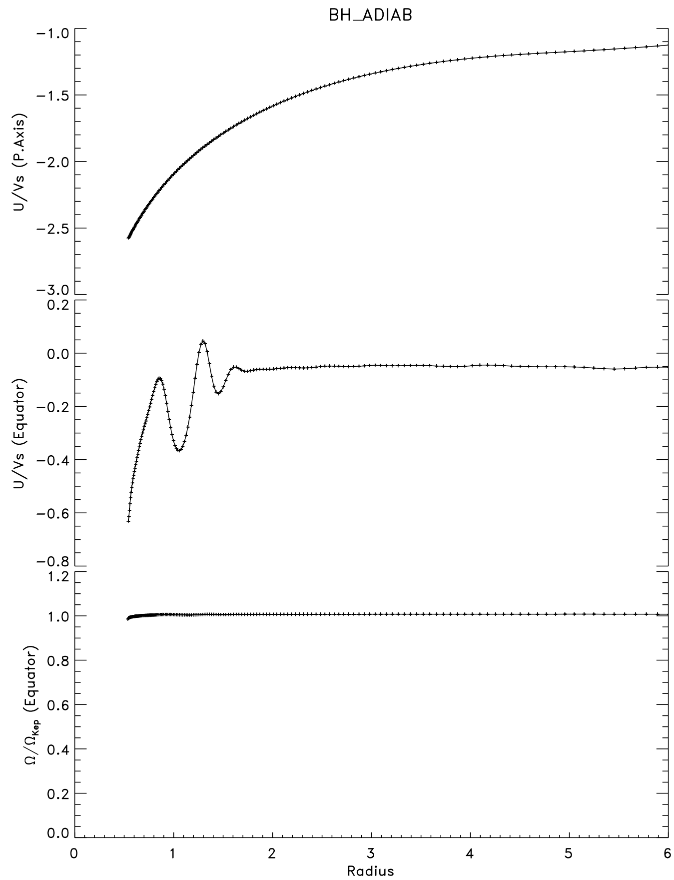

Fig. 2. Profiles of Mach numbers along the polar axis (top), along the equator (middle) and the ratio of the angular velocity to the keplerian along the equator (bottom). In this model turbulent heating and cooling are set to equalize locally (see Fig. 1).

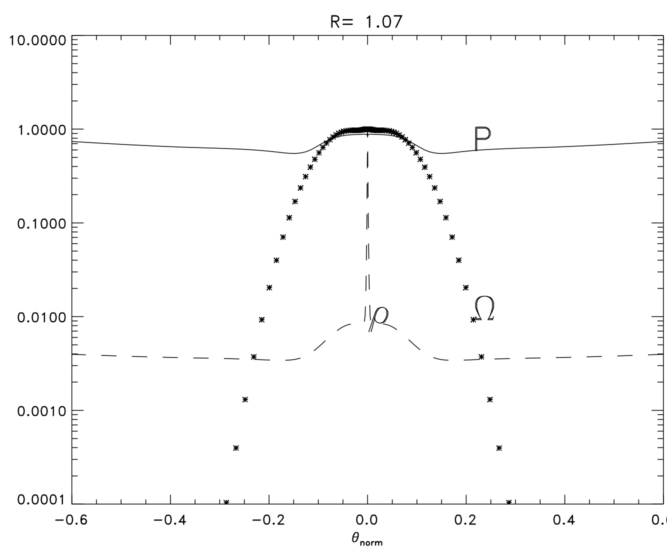

Fig. 3. Profiles of the normalized density, angular velocity and pressure along constant radius ($R = R_{\rm ms}$) after 2000 orbital periods. The latitude is normalized to $\pi/2$. In this model turbulent heating and cooling via Bremsstrahlung are activated.

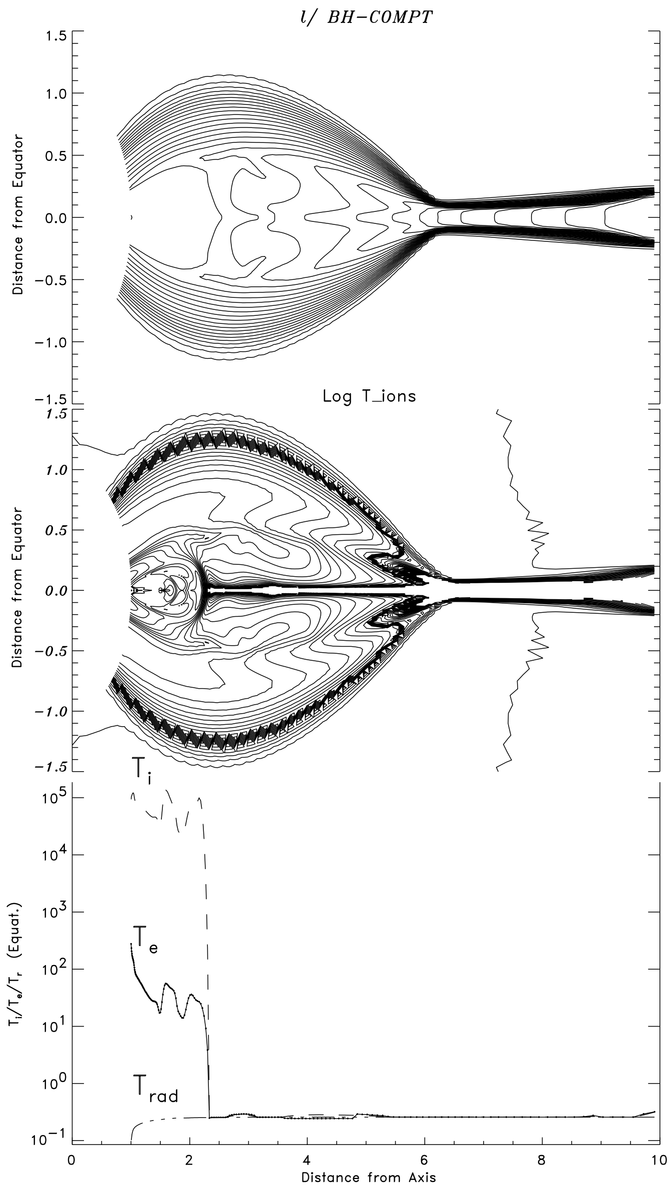

Fig. 4. 35 equi-distant iso-lines of the specific angular momentum ℓ (top) and the ion-temperature T_i (middle) after 150 orbital periods (at the marginal stable radius). The decoupling of the ion–temperature T_i from the electron temperature T_e and the radiative temperature T_rad (in units of 5×10^7K) in the inner region at radii $\leq 2.3\,R_\mathrm{in} = 6.5\,R_\mathrm{S}$ is obvious (bottom). In this model, turbulent heating and cooling via Bremsstrahlung and comptonization are included. In this computation, the results from the Bremsstrahlung model are used as starting configuration (Fig. 5)

Acknowledgements. AH's research has been supported by the Deutsche Forschungsgemeinschaft (DFG) through the Schwerpunktprogramm *Physik der Sternenentstehung*. Computations were performed on facilities provided by Interdisciplinary Center for Scientific Computing (IWR) at the University of Heidelberg.

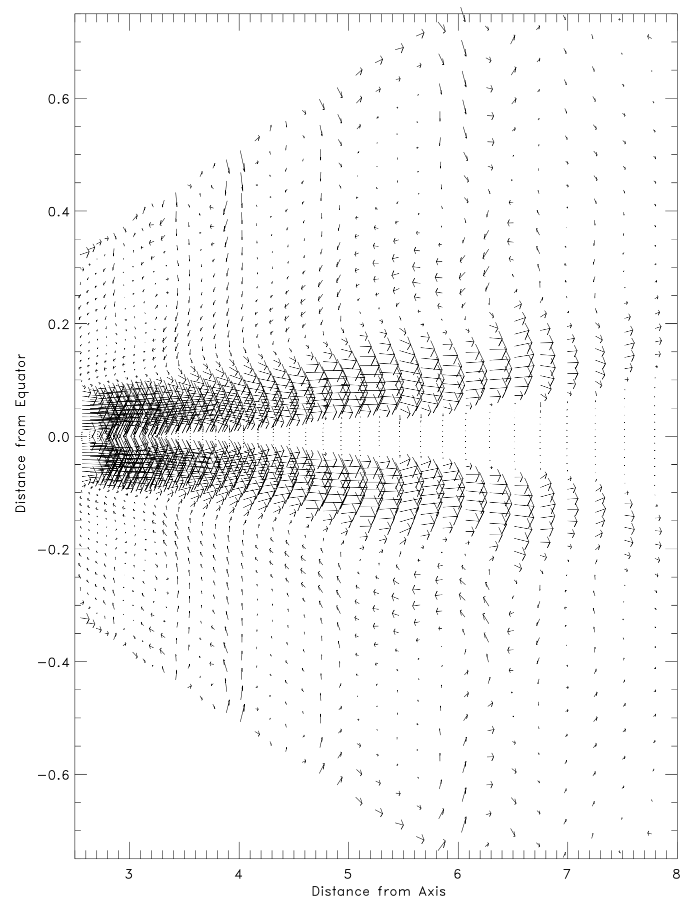

Fig. 5. The structure of the velocity field in the disk (left) and near the inner radius (right). The convective energy transport from the disk to higher latitudes is obvious (left). This model calculation includes viscous dissipation and cooling by Bremsstrahlung (as in Fig. 3).

References

Abramowicz, M., Lasota, J-P, Igumenshchev, I.V., 2000, MNRAS, 314, 775
Blandford, R., Begelman, M.C, 1999, MNRAS,303, L1
Hawley, J.F., 2000, ApJ, 528, 462
Hujeirat, A., 1998, MNRAS, 298, 320
Hujeirat, A., Camenzind, M., 2000, in preparation
Igumenshchev,I.V., Abramowicz, M.A., Narayan, R., 2000, ApJ, 537L, 27
Igumenshchev,I.V., Abramowicz, M.A., 2000, Astro-ph/0003397
Narayan, R., Yi, I., 1994, ApJ, 428, L13
Pomraning, G.C, Levermore, C.D., 1981, ApJ, 248, 321
Paczynski, B., Wiita, P.J., 1980, A&A, 88, 23
Różańska, A., Czerny, B., 2000, Astro-ph/0004158
Shapiro, S.L., Lightman A.P., Eardley, D.M., 1976, ApJ, 204, 187 (SLE)
Rees, M.J., Begelman, M.C., Blandford, R., Phinney E.S., 1982, Nat, 295, 17